We are IntechOpen,
the world's leading publisher of
Open Access books
Built by scientists, for scientists

6,900
Open access books available

186,000
International authors and editors

200M
Downloads

Our authors are among the

154
Countries delivered to

TOP 1%
most cited scientists

12.2%
Contributors from top 500 universities

WEB OF SCIENCE™

Selection of our books indexed in the Book Citation Index
in Web of Science™ Core Collection (BKCI)

Interested in publishing with us?
Contact book.department@intechopen.com

Numbers displayed above are based on latest data collected.
For more information visit www.intechopen.com

Adaptive Filtering Using Subband Processing: Application to Background Noise Cancellation

Ali O. Abid Noor, Salina Abdul Samad and Aini Hussain
The National University of Malaysia (UKM),
Malaysia

1. Introduction

Adaptive filters are often involved in many applications, such as system identification, channel estimation, echo and noise cancellation in telecommunication systems. In this context, the Least Mean Square (LMS) algorithm is used to adapt a Finite Impulse Response (FIR) filter with a relatively low computation complexity and good performance. However, this solution suffers from significantly degraded performance with colored interfering signals, due to the large eigenvalue spread of the autocorrelation matrix of the input signal (Vaseghi, 2008). Furthermore, as the length of the filter is increased, the convergence rate of the algorithm decreases, and the computational requirements increase. This can be a problem in acoustic applications such as noise cancellation, which demand long adaptive filters to model the noise path. These issues are particularly important in hands free communications, where processing power must be kept as low as possible (Johnson et al., 2004). Several solutions have been proposed in literature to overcome or at least reduce these problems. A possible solution to reduce the complexity problem has been to use adaptive Infinite Impulse Response (IIR) filters, such that an effectively long impulse response can be achieved with relatively few filter coefficients (Martinez & Nakano 2008). The complexity advantages of adaptive IIR filters are well known. However, adaptive IIR filters have the well known problems of instability, local minima and phase distortion and they are not widely welcomed. An alternative approach to reduce the computational complexity of long adaptive FIR filters is to incorporate block updating strategies and frequency domain adaptive filtering (Narasimha 2007; Wasfy & Ranganathan, 2008). These techniques reduce the computational complexity, because the filter output and the adaptive weights are computed only after a large block of data has been accumulated. However, the application of such approaches introduces degradation in the performance, including a substantial signal path delay corresponding to one block length, as well as a reduction in the stable range of the algorithm step size. Therefore for nonstationary signals, the tracking performance of the block algorithms generally becomes worse (Lin et al., 2008).

As far as speed of convergence is concerned, it has been suggested to use the Recursive Least Square (RLS) algorithm to speed up the adaptive process (Hoge et al., 2008).The convergence rate of the RLS algorithm is independent of the eigenvalue spread. Unfortunately, the drawbacks that are associated with RLS algorithm including its $O(N^2)$ computational requirements, which are still too high for many applications, where high

speed is required, or when a large number of inexpensive units must be built. The Affine Projection Algorithm (APA) (Diniz, 2008; Choi & Bae, 2007) shows a better convergence behavior, but the computational complexity increases with the factor P in relation to LMS, where P denotes the order of the APA.

As a result, adaptive filtering using subband processing becomes an attractive option for many adaptive systems. Subband adaptive filtering belongs to two fields of digital signal processing, namely, adaptive filtering and multirate signal processing. This approach uses filter banks to split the input broadband signal into a number of frequency bands, each serving as an independent input to an adaptive filter. The subband decomposition is aimed to reduce the update rate, and the length of the adaptive filters, hopefully, resulting in a much lower computational complexity. Furthermore, subband signals are usually downsampled in a multirate system. This leads to a whitening of the input signals and therefore an improved convergence behavior of the adaptive filter system is expected. The objectives of this chapter are: to develop subband adaptive structures which can improve the performance of the conventional adaptive noise cancellation schemes, to investigate the application of subband adaptive filtering to the problem of background noise cancellation from speech signals, and to offer a design with fast convergence, low computational requirement, and acceptable delay. The chapter is organized as follows. In addition to this introduction section, section 2 describes the use of Quadrature Mirror Filter (QMF) banks in adaptive noise cancellation. The effect of aliasing is analyzed and the performance of the noise canceller is examined under various noise environments. To overcome problems incorporated with QMF subband noise canceller system, an improved version is presented in section 3. The system is based on using two-fold oversampled filter banks to reduce aliasing distortion, while a moderate order prototype filter is optimized for minimum amplitude distortion. Section 4 offers a solution with reduced computational complexity. The new scheme is based on using polyphase allpass IIR filter banks at the analysis stage, while the synthesis filter bank is optimized such that an inherent phase correction is made at the output of the noise canceller. Finally, section 5 concludes the chapter.

2. Adaptive noise cancellation using QMF banks

In this section, a subband adaptive noise canceller system is presented. The system is based on using critically sampled QMF banks in the analysis and synthesis stages. A suband version of the LMS algorithm is used to control a FIR filter in the individual branches so as to reduce the noise in the input noisy signal.

2.1 The QMF bank

The design of M-band filter bank is not quite an easy job, due to the downsampling and upsampling operations within the filter bank. Therefore, iterative algorithms are often employed to optimize the filter coefficients (Bergen 2008; Hameed et al. 2006). This problem is simplified for the special case where $M = 2$ which leads to the QMF bank as shown in Fig.1. Filters $H_0(z)$ and $G_0(z)$ are lowpass filters and $H_1(z)$ and $G_1(z)$ are highpass filters with a nominal cut off of $\frac{f_s}{4}$ or $\frac{\pi}{2}$, where f_s is the sampling frequency.
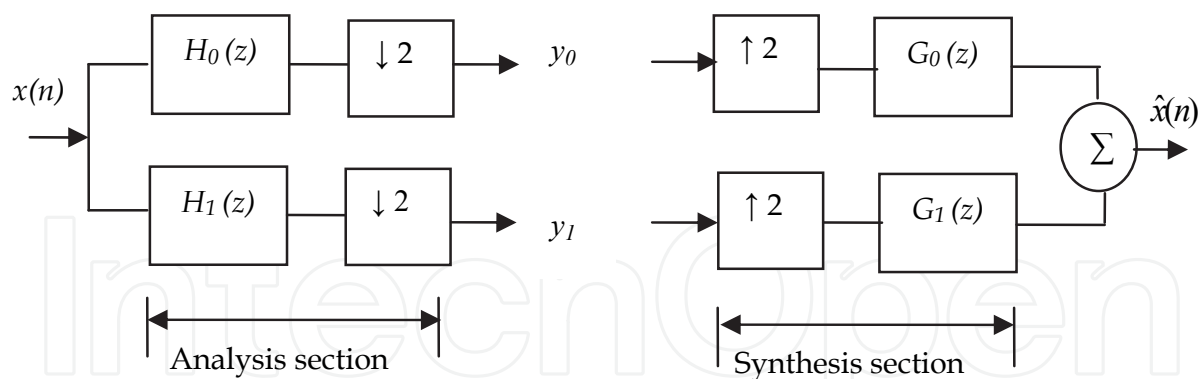
Fig. 1. The quadrature mirror filter (QMF) bank

The downsampling operation has a modulation effect on signals and filters, therefore the input to the system is expressed as follows;

$$\mathbf{X}(z) = [X(z) \quad X(-z)]^T \tag{1}$$

where $.^T$ is a transpose operation. Similarly, the analysis filter bank is expressed as,

$$\mathbf{H}(z) = \begin{bmatrix} H_0(z) & H_0(-z) \\ H_1(z) & H_1(-z) \end{bmatrix} \tag{2}$$

The output of the analysis stage is expressed as,

$$\mathbf{Y}(z) = \mathbf{H}(z)\mathbf{X}(z) \tag{3}$$

The total input-output relationship is expressed as,

$$\hat{X}(z) = \frac{1}{2}X(z)\big[H_0(z)G_0(z) + H_1(z)G_1(z)\big] + \frac{1}{2}X(-z)\big[H_0(-z)G_0(z) + H_1(-z)G_1(z)\big] \tag{4}$$

The right hand side term of equation (4) is the aliasing term. The presence of aliasing causes a frequency shift of π in signal argument, and it is unwanted effect. However, it can be eliminated by choosing the filters as follows;

$$H_1(z) = H_0(-z) \tag{6}$$

$$G_0(z) = H_0(z) \tag{7}$$

$$G_1(z) = -H_0(-z) \tag{8}$$

By direct substitution into Equation (4), we see that the aliasing terms go to zero, leaving

$$\hat{X}(z) = \frac{1}{2}X(z)\Big[H_0^2(z) + H_1^2(z)\Big] \tag{9}$$

In frequency domain, replacing z by $e^{j\omega}$, where $\omega = 2\pi f$, equation (9) can be expressed as,

$$\hat{X}(e^{j\omega}) = \frac{1}{2} X(e^{j\omega}) \left[H_0^2(e^{j\omega}) + H_1^2(^{j\omega}) \right] \qquad (10)$$

Therefore, the objective is to determine $H_0^2(e^{j\omega})$ such that the overall system frequency approximates $e^{j\omega . n_0}$, i.e. approximates an allpass function with constant group delay n_0. All four filters in the filter bank are specified by a length L lowpass FIR filter.

2.2 Efficient implementation of the QMF bank

An efficient implementation of the preceding two-channel QMF bank is obtained using polyphase decomposition and the noble identities (Milic, 2009). Thus, the analysis and synthesis filter banks can be redrawn as in Fig.2. The downsamplers are now to the left of the polyphase components of $H_0(z)$, namely $F_0(z)$ and $F_1(z)$, so that the entire analysis bank requires only about $L/2$ multiplications per unit sample and $L/2$ additions per unit sample, where L is the length of $H_0(z)$.
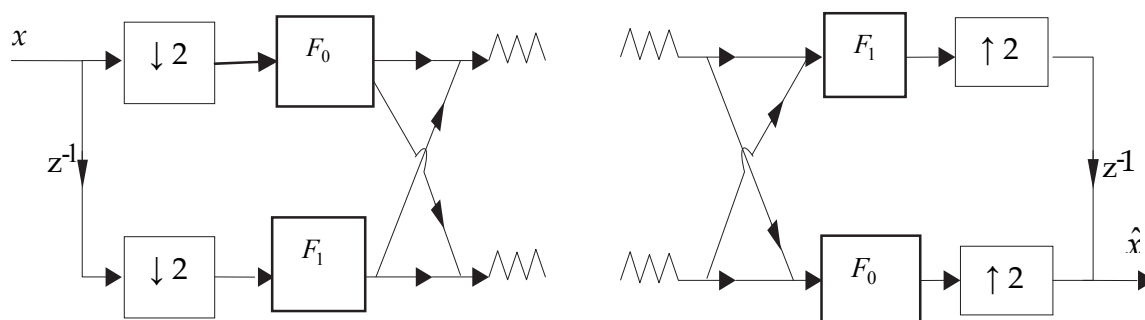

Fig. 2. Polyphase implementation of QMF bank

2.3 Distortion elimination in QMF banks

Let the input-output transfer function be $T(z)$, so that

$$T(z) = \frac{\hat{x}(z)}{x(z)} = \frac{1}{2} \left[H_0(z)G_0(z) + H_1(z)G_1(z) \right] \qquad (11)$$

which represents the distortion caused by the QMF bank. $T(z)$ is the overall transfer function (or the distortion transfer function). The processed signal $\hat{x}(n)$ suffers from amplitude distortion if $\left| T(e^{j\omega}) \right|$ is not constant for all ω, and from phase distortion if $T(z)$ does not have linear phase. To eliminate amplitude distortion, it is necessary to constrain $T(z)$ to be allpass, whereas to eliminate phase distortion, we have to restrict $T(z)$ to be FIR with linear phase. Both of these distortions are eliminated if and only if $T(z)$ is a pure delay, i.e.

$$T(z) = cz^{n_0} \qquad (12)$$

where c is a scalar constant, or, equivalently,

$$\hat{x}(n) = cx(n - n_0) \qquad (13)$$

Systems which are alias free and satisfy (12) are called perfect reconstruction (PR) systems. For any pair of analysis filter, the choice of synthesis filters according to (7) and (8) eliminates aliasing distortion, the distortion can be expressed as,

$$T(z)\frac{1}{2}\left[H_0(z)H_1(-z) + H_1(z)H_0(z)\right] \tag{14}$$

The transfer function of the system in (14) can be expressed in terms of polyphase components as,

$$T(z) = \frac{1}{2}\left[H_0^2(z) - H_0^2(-z)\right] = 2z^{-1}F_0(z^2)F_1(z^2) \tag{15}$$

Since $H_0(z)$ is restricted to be FIR, this is possible if and only if $F_0(z)$ and $F_1(z)$ are delays, which means $H_0(z)$ must have the form;

$$H_0(z) = c_0 z^{-2n_0} + c_1 z^{-(2n_1+1)} \tag{16}$$

For our purpose of adaptive noise cancellation, frequency responses are required to be more selective than (16). So, under the constraint of (13), perfect reconstruction is not possible. However, it is possible to minimize amplitude distortion by optimization procedures. The coefficients of $H_0(z)$ are optimized such that the distortion function is made as flat as possible. The stopband energy of $H_0(z)$ is minimized, starting from the stopband frequency. Thus, an objective function of the form

$$\beta \int_{\omega s}^{\pi} \left|H_0(e^{j\omega})\right|^2 d\omega + (1-\beta)\int_0^{\pi/2} [1 - \left|T(e^{j\omega})\right|^2]^2 d\omega \tag{17}$$
$$0 < \beta < 1$$

can be minimized by optimizing the coefficients of $H_0(z)$. The factor β is used to control the tradeoff between the stopband energy of $H_0(z)$ and the flatness of $\left| T(e^{j\omega}) \right|$. The prototype filter $H_0(z)$ is constraint to have linear phase if $T(z)$ must have a linear phase. Therefore, the prototype filter $H_0(z)$ is chosen to be linear phase FIR filter with L=32 .

2.4 Adaptive noise cancellation using QMF banks

A schematic of the two-band noise canceller structure is shown at Fig.3, this is a two sensor scheme, it consists of three sections: analysis which contains analysis filters $H_0(z)$, $H_1(z)$ plus the down samplers, adaptive section contains two adaptive FIR filters with two controlling algorithms, and the synthesis section which comprises of two upsamplers and two interpolators $G_0(z)$, $G_1(z)$. The noisy speech signal is fed from the primary input, whilst, the noise $\hat{x}$ is fed from the reference input sensor, $\hat{x}$ is added to the speech signal via a transfer function $A(z)$ which represents the acoustic noise path, thus $\hat{x}$ correlated with x and uncorrelated with s. In stable conditions, the noise x should be cancelled completely leaving the clean speech as the total error signal of the system. The suggested two channel adaptive

noise cancellation scheme is shown in Fig.3. It is assumed in this configuration that z transforms of all signals and filters exist on the unit circle. Thus, from Fig. 3, we see that the noise $X(z)$ is filtered by the noise path $A(z)$. The output of $A(z)$, $\hat{X}(z)$ is added to the speech signal, $S(z)$, and it is then split by an analysis filter bank $H_0(z)$ and $H_1(z)$ and subsampled to yield the two subband system signals V_0 and V_1. The adaptive path first splits the noise $X(z)$ by an identical analysis filter bank, and then models the system in the subband domain by two independent adaptive filters, yield to the two estimated subband signals y_0 and y_1. The subband error signals are obtained as,

$$E_k(z) = V_k(z) - Y_k(z), \quad \text{for } k = 0,1 \tag{18}$$

The system output $\hat{S}$ is obtained after passing the subband error signals e_0 and e_1 through a synthesis filter bank $G_0(z)$ and $G_1(z)$. The subband adaptive filter coefficients $\hat{\mathbf{w}}_0$ and $\hat{\mathbf{w}}_1$ have to be adjusted so as to minimize the noise in the output signal, in practice, the adaptive filters are adjusted so as to minimize the subband error signals e_0 and e_1.
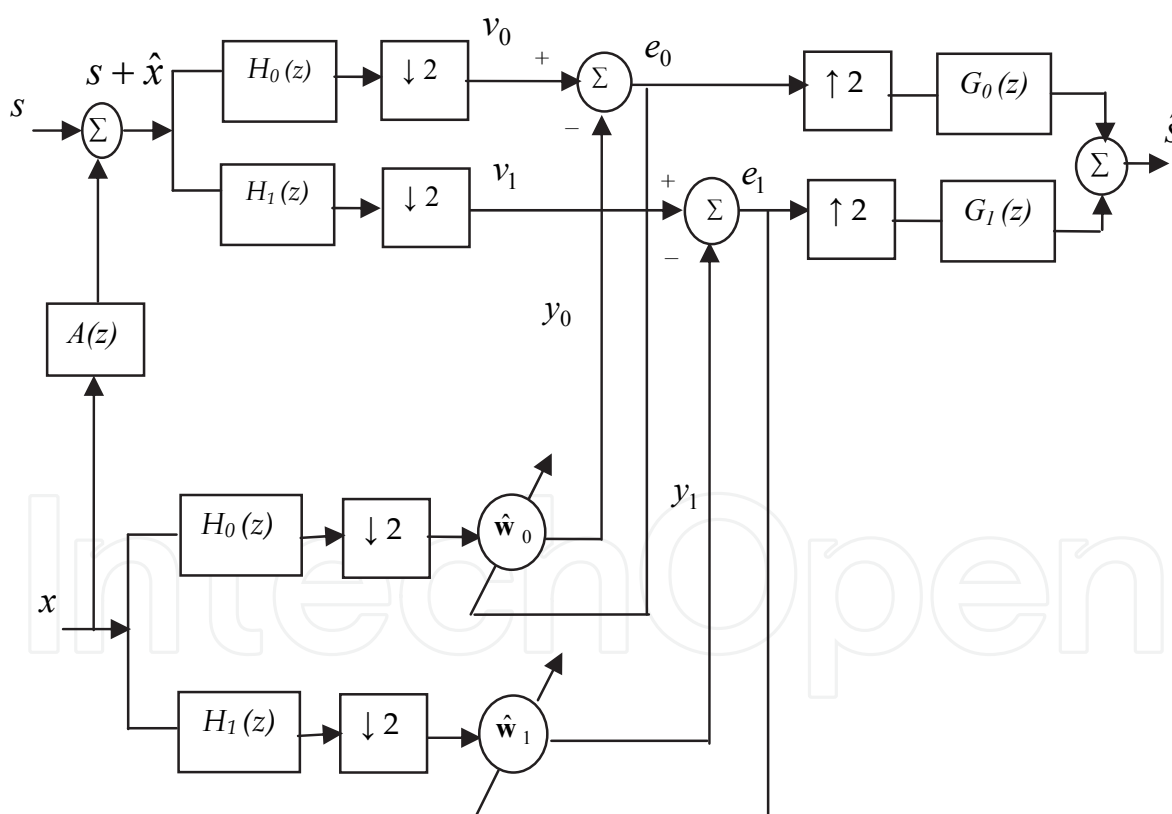

Fig. 3. The two-band noise canceller

In the adaptive section of the two-band noise canceller, a modified version of the LMS algorithm for subband adaptation is used as follows;

$$J(\hat{\mathbf{w}}) = e_0^2(n) + e_1^2(n) \tag{19}$$

where $J(\hat{w})$ is a cost function which depends on the individual errors of the two adaptive filters. Taking the partial derivatives of $J(\hat{w})$ with respect to the samples of $\hat{w}$, we get the components of the instantaneous gradient vector. Then, the LMS adaptation algorithm is expressed in the form;

$$\hat{w}_i(n) = \hat{w}_i(n-1) - \mu(n)\left[2e_0(n)\frac{\partial e_0(n)}{\partial \hat{w}_i} + 2e_1(n)\frac{\partial e_1(n)}{\partial \hat{w}_i}\right] \tag{20}$$

for $i=0,1,2\ldots L_w-1$, where L_w is the length of the branch adaptive filter. The convergence of the algorithm (20) towards the optimal solution $s = \hat{s}$ is controlled by the adaptation step size μ. It can be shown that the behavior of the mean square error vector is governed by the eigenvalues of the autocorrelation matrix of the input signal, which are all strictly greater than zero (Haykin, 2002). In particular, this vector converges exponentially to zero provided that $\mu < 1/\lambda_{\max}$, where $\lambda_{\max}$ is the largest eigenvalue of the input autocorrelation matrix. This condition is not sufficient to insure the convergence of the Mean Square Error (MSE) to its minimum. Using the classical approach , a convergence condition for the MSE is stated as

$$\mu < \frac{2}{trR} = \mu_{\max} \tag{21}$$

where trR is the trace of the input autocorrelation matrix R.

2.5 The M-band case

The two-band noise canceller can be extended so as to divide the input broadband signal into M bands, each subsampled by a factor of M. The individual filters in the analysis bank are chosen as a bandpass filters of bandwidth f_s/M (if the filters are real, they will have two conjugate parts of bandwidth $f_s/2M$ each). Furthermore, it is assumed that the filters are selective enough so that they overlap only with adjacent filters. A convenient class of such filters which has been studied for subband coding of speech is the class of pseudo-QMF filters (Deng et al. 2007). The *kth* filter of such a bank is obtained by cosine modulation of a low-pass prototype filter with cutoff frequency $f_s/4M$. For our purpose of noise cancellation, the analysis and synthesis filter banks are made to have a paraunitary relationship so as the following condition is satisfied.

$$\frac{1}{M}\sum_{k=0}^{M-1} G_k(z)H_k(zW_M^{-i}) = cz^{-\tau} \tag{22}$$

where c is a constant, W_M is the Mth root of unity, with $i=0,1,2,\ldots M-1$ and τ is the analysis/synthesis reconstruction delay. Thus, the prototype filter order partly defines the signal delay in the system. The above equation is the perfect reconstruction (PR) condition in z-transform domain for causal M-channel filter banks. The characteristic feature of the paraunitary filter bank is the relation of analysis and synthesis subfilters; they are connected via time reversing. Then, the same PR-condition can be written as,

$$\frac{1}{M}\sum_{k=0}^{M-1} H_k(z^{-1})H_k(zW_M^{-i}) = cz^{-\tau} \tag{23}$$

The reconstruction delay of a paraunitary filter bank is fixed by the prototype filter order, $\tau = L$, where L is the order of the prototype filter. Amplitude response for such a filter bank is shown in Fig.4. The analysis matrix in (2) can be expressed for the M-band case as,

$$\mathbf{H}(z) = \begin{bmatrix} H_0(z) & H_0(zW) & \dots & H_0(zW^{M-1}) \\ H_1(z) & H_1(zW) & \dots & H_1(zW^{M-1}) \\ \vdots & & & \\ H_{M-1}(z) & H_{M-1}(zW) & \dots & H_{M-1}(zW^{M-1}) \end{bmatrix} \tag{24}$$

The matrix in (24) contains the filters and their modulated versions (by the Mth root of unity $W = e^{-j2\pi/M}$). This shows that there are M-1 alias components $H(zW^k)$, $k > 0$ in the reconstructed signal.
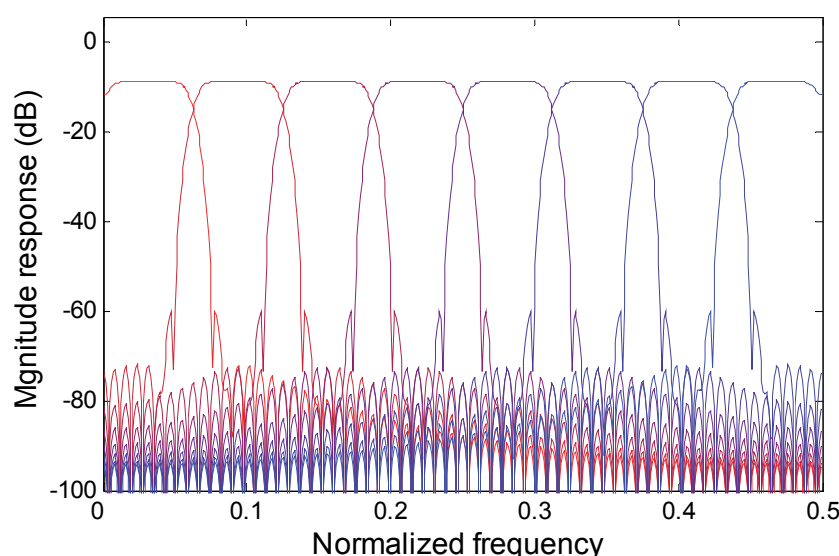
Fig. 4. Magnitude response of 8-band filter bank, with prototype order of 63

2.6 Results of the subband noise canceller using QMF banks
2.6.1 Filter bank setting and distortion calculation

The analysis filter banks are generated by a cosine modulation function. A single prototype filter is used to produce the sub-filters in the critically sampled case. Aliasing error is the parameter that most affect adaptive filtering process in subbands, and the residual noise at the system's output can be very high if aliasing is not properly controlled. Fig.5 gives a describing picture about aliasing distortion. In this figure, settings of prototype filter order are used for each case to investigate the effect of aliasing on filter banks. It is clear from Fig.5, that aliasing can be severe for low order prototype filters. Furthermore, as the number of subbands is increased, aliasing insertion is also increased. However, for low number of subbands e.g. 2 subbabds, low order filters can be afforded with success equivalent to high order ones.

2.6.2 Noise cancellation tests

Initially, the two-band noise canceller model is tested using a variable frequency sine wave contaminated with zero mean, unit variance white Gaussian noise. This noise is propagating through a noise path $A(z)$, applied to the primary input of the system. The same Gaussian noise is passed directly to the reference input of the canceller. Table 1 lists the various parameters used in the experiment.
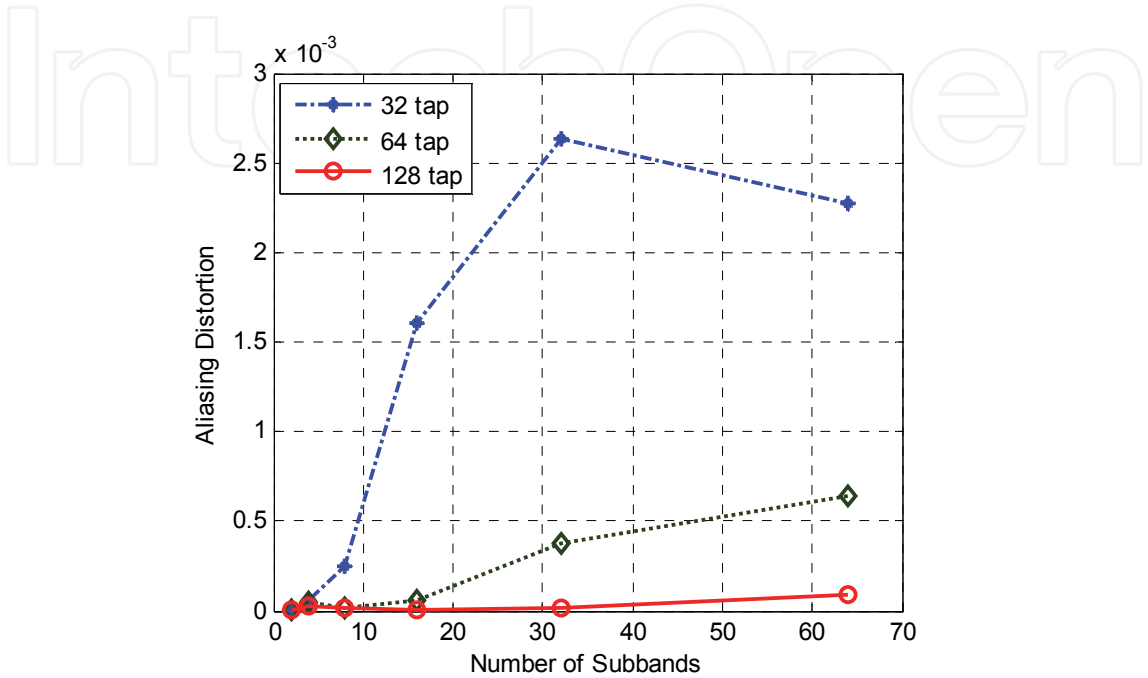

Fig. 5. Aliasing versus the number of subbands for different prototype filter length

Parameter	Value
Noise path length	92
Adaptive filter length	46
Step size μ	0.02
Sampling frequency	8kHz
Input (first test)	Variable frequency sinusoid
Noise (first test)	Gaussian white noise with zero mean and unit variance
Input (second test)	Speech of a woman
Noise (second test)	Machinery noise

Table 1. Test parameters

In a second experiment, a speech of a woman, sampled at 8 kHz, is used for testing. Machinery noise as an environmental noise is used to corrupt the speech signal. Convergence behavior using mean square error plots are used as a measure of performance. These plots are smoothed with 200 point moving average filter and displayed as shown in Fig.6 for the case of variable frequency sine wave corrupted by white Gaussian noise, and in Fig.7 for the case speech input corrupted by machinery noise.
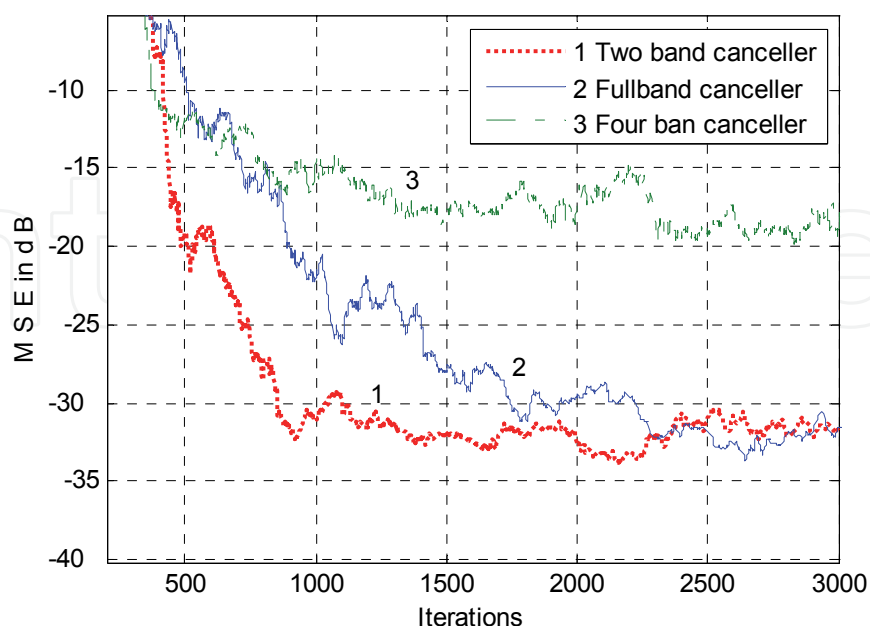
Fig. 6. MSE performance under white environment

2.7 Discussion

The use of the two-band QMF scheme, with near perfect reconstruction filter bank, should lead to approximately zero steady state error at the output of the noise cancellation scheme; this property has been experimentally verified as shown in Fig.6. The fullband adaptive filter performance as well as for a four-band critically sampled scheme are shown on the same graph for sake of comparison. The steady state error of the scheme with two-band QMF banks is very close to the error of the fullband filter, this demonstrate the perfect identification property. Those results show that the adaptive filtering process in subbands based on the feedback of the subbands errors is able to model perfectly a system. The subband plots exhibit faster initial parts; however, after the error has decayed by about 15 dB (4-band) and 30 dB (2-band), the convergence of the four-band scheme slows down dramatically. The errors go down to asymptotic values of about -30 dB (2-band) and -20 dB (4-band). The steady state error of the four-band system is well above the one of the fullband adaptive filter due to high level of aliasing inserted in the system. The improvement of the transient behavior of the four-band scheme was observed only at the start of convergence. The aliased components in the output error cannot be cancelled, unless cross adaptive filters are used to compensate for the overlapping regions between adjacent filters, this would lead to an even slower convergence and an increase in computational complexity of the system. Overall, the convergence performances of the two-band scheme are significantly better than that of the four-band scheme: in particular, the steady state error is much smaller. However, the convergence speed is not improved as such, in comparison with the fullband scheme. The overall convergence speed of the two-band scheme was not found significantly better than the one of the fullband adaptive filter. Nevertheless, such schemes would have the practical advantage of reduced computational complexity in comparison with the fullband adaptive filter.
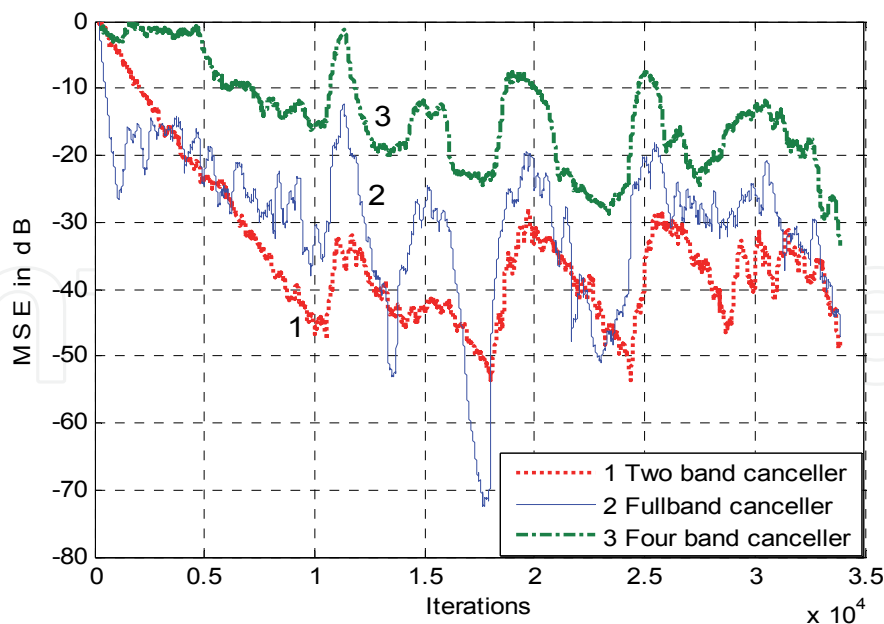
Fig. 7. MSE performance under white environment

3. Adaptive noise cancellation using optimized oversampled filter banks

Aliasing insertion in the critically sampled systems plays a major role in the performance degradation of subband adaptive filters. Filter banks can be designed alias-free and perfectly reconstructed when certain conditions are met by the analysis and synthesis filters. However, any filtering operation in the subbands may cause a possible phase and amplitude change and thereby altering the perfect reconstruction property. In a recent study, Kim et al. (2008) have proposed a critically sampled structure to reduce aliasing effect. The inter-band aliasing in each subband is obtained by increasing the bandwidth of a linear-phase FIR analysis filter, and then subtracted from the subband signal. This aliasing reduction technique introduces spectral dips in the subband signals. Therefore, extra filtering operation is required to reduce these dips.

In this section, an optimized 2-fold oversampled M-band noise cancellation technique is used to mitigate the problem of aliasing insertion associated with critically sampled schemes. The application to the cancellation of background noise from speech signals is considered. The prototype filter is obtained through optimization procedure. A variable step size version of the LMS algorithm is used to control the noise in the individual branches of the proposed canceller. The system is implemented efficiently using polyphase format and FFT/IFFT transforms. The proposed scheme offers a simplified structure that without employing cross-filters or gap filter banks reduces the aliasing level in the subbands. The issue of increasing initial convergence rate is addressed. The performance under white and colored environments is evaluated and compared to the conventional fullband method as well as to a critically sampled technique developed by Kim et al. (2008). This evaluation is offered in terms of MSE convergence of the noise cancellation system.

3.1 Problem formulation

The arrangement in Fig.3 is redrawn for the general case of M-band system downsampled with a factor of D as shown in Fig.8.
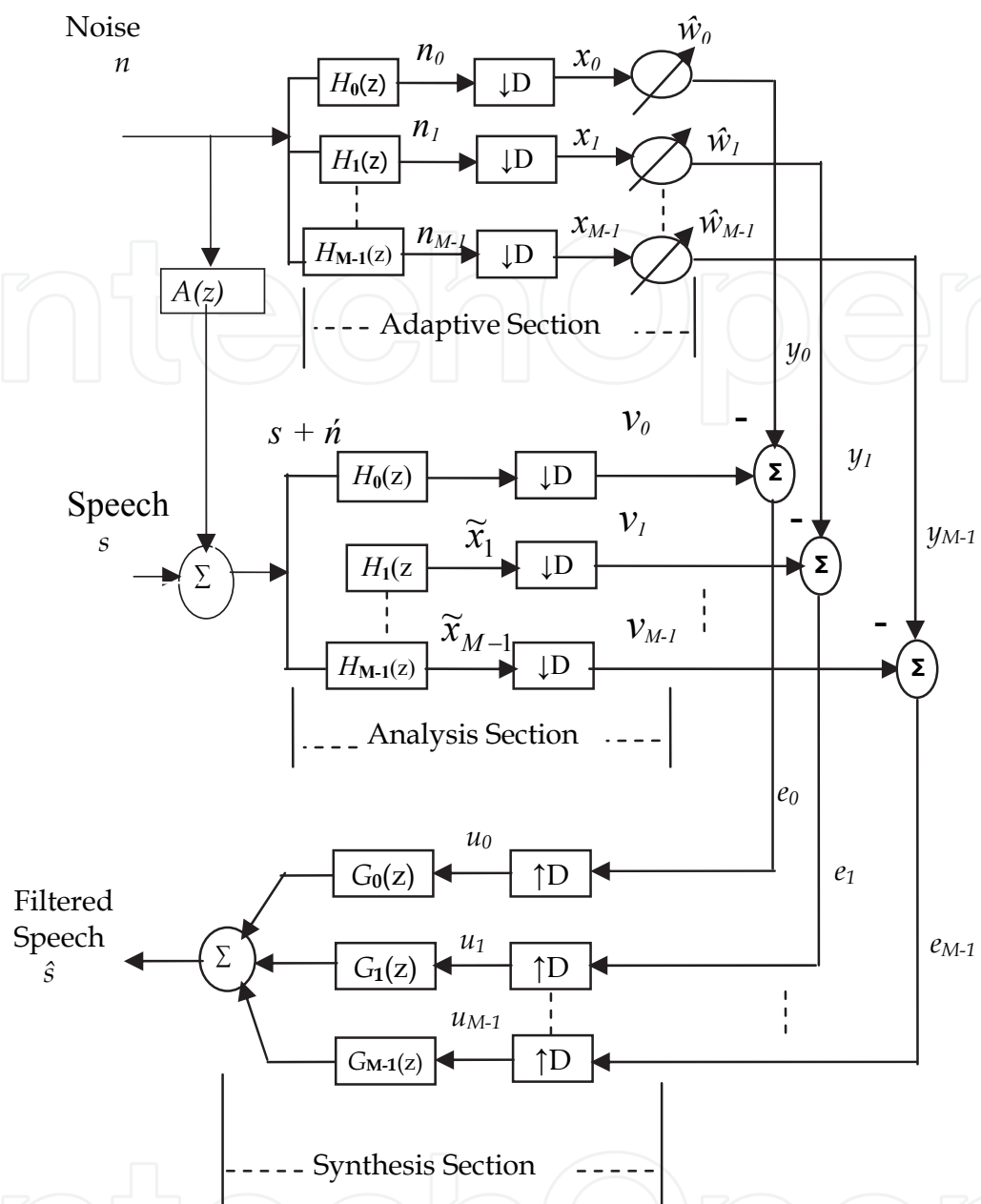
Fig. 8. The M-band noise canceller with downsampling factor set to D

Distortions due the insertion of the analysis/synthesis filter bank are expressed as follows,

$$T_0(z) \approx \frac{1}{M} \sum_{k=0}^{M-1} G_K(z)H_k(z) \tag{25}$$

$$T_i(z) \approx \frac{1}{D} \sum_{k=0}^{M-1} G_K(z)H_k(zW_D^l) \quad , \text{for} \quad i=1,2,.....D-1 \tag{26}$$

A critical sampling creates severe aliasing effect due to the transition region of the prototype filter. This has been discussed in section 2. When the downsampling factor decreases, the aliasing effect is gradually reduced. Optimizing the prototype filter by minimizing both

$T_0(z)$ and $T_i(z)$ may result in performance deviated toward one of them. Adjusting such an optimization process is not easy in practice, because there are two objectives in the design of the filter bank. Furthermore, minimizing aliasing distortion $T_i(z)$ using the distortion function $T_0(z)$ as a constraint is a very non-linear optimization problem and the results may not reduce both distortions. Therefore, in this section, we use 2-times oversampling factor to reduce aliasing error, and the total system distortion is minimized by optimizing a single prototype filter in the analysis and synthesis stages. The total distortion function $T_0(z)$ and the aliasing distortion $T_i(z)$ can be represented in frequency domain as,

$$T_0(e^{j\omega}) \approx \frac{1}{M} \sum_{k=0}^{M-1} G_K(e^{j\omega}) H_k(e^{j\omega})$$

(27)

$$T_i(e^{j\omega}) \approx \frac{1}{D} \sum_{k=0}^{M-1} G_K(e^{j\omega}) H_k(e^{j\omega} W_D^l)$$

(28)

The objective is to find prototype filters $H_0(e^{j\omega})$, and $G_0(e^{j\omega})$, that minimize the system reconstruction error. In effect, a single lowpass filter is used as a prototype to produce the analysis and synthesis filter banks by Discrete Fourier Transform (DFT) modulation,

$$H_k(z) = H_0(ze^{2\pi k/M})$$

(25)

3.2 Prototype filter optimization

Recalling that, the objective here is to find prototype filter $H_0(e^{j\omega})$ to minimize reconstruction error. In frequency domain the analysis prototype filter is given by

$$H_0(e^{j\omega}) = \sum_{n=0}^{L-1} h_0(n) e^{-j\omega n}$$

(29)

For a lowpass prototype filter whose stop-band stretches from ω_s to π, we minimize the total stopband energy according to the following function

$$E_s = \int_{\omega_s}^{\pi} \left| H_0(e^{j\omega}) \right|^2 d\omega$$

(30)

For M-channel filter banks the stopband edge is expressed as,

$$\omega_s = \frac{\pi(1+\beta)}{2M}$$

(31)

where β is the roll-off parameter. Stopband attenuation is the measure that is used when comparing the design results with different parameters. The numerical value is the highest sidelobe given in dBs when the prototype filter passband is normalized to 0 dB. E_s is expressed with a quadratic matrix as follows;

$$E_s = \mathbf{h}^T \mathbf{\Phi} \mathbf{h}$$

(32)

where vector $\mathbf{h}$ contains the prototype filter impulse response coefficients, and $\mathbf{\Phi}$ is given by Nguyen (1993) as,

$$\Phi_{n,m} = \begin{cases} \pi - \omega_s & n = m \\ \dfrac{1}{n-m}(\sin((n-m)\pi) - \sin((n-k)\omega_s)) & n \neq m \end{cases} \tag{33}$$

The optimum coefficients of the FIR filter are those that minimize the energy function E_s in (30). For M-band complementary filter bank, the frequency $\omega = \pi / 2M$ is located at the middle of the transition band of its prototype filter. The pass-band covers the frequency range of $0 \leq \omega \leq \dfrac{\pi(1-\beta)}{2M}$. For a given number of subbands, M, a roll-off factor β and for a certain length of prototype filter L we find the optimum coefficients of the FIR filter. The synthesis prototype filter $G_0(e^{j\omega})$, is a time reversed version of $H_0(e^{j\omega})$. In general, it is not easy to maintain the low distortion level unless the length of the filter increases to allow for narrow transition regions. The optimization is run for various prototype filter lengths L, different number of subbands M and certain roll-off factors β. Frequency response of the final design of prototype filter is shown in Fig.9.

3.3 The adaptive process
The filter weight updating is performed using a subband version of the LMS algorithm that is expressed by the following;

$$\hat{\mathbf{w}}_k(m+1) = \hat{\mathbf{w}}_k(m) + \mu_k.\alpha_k.e_k(m)\mathbf{x}_k(m) \tag{34}$$

$$e_k(m) = v_k(m) - y_k(m) \tag{35}$$

$$y_k(m) = \hat{\mathbf{w}}_k^{T}(m)\mathbf{x}_k(m) \tag{36}$$

The filter weights in each branch are adjusted using the subband error signal belonging to the same branch. To prevent the adaptive filter from oscillating or being too slow, the step size of the adaptation algorithm is made inversely proportional to the power in the subband signals such that

$$\alpha_k = \frac{1}{\sigma + \|x_k\|^2} \tag{37}$$

where $\|x_k\|$ is the norm of the input signal and σ is a small constant used to avoid possible division by zero. On the other hand, a suitable value of the adaptation gain factor μ is deduced using trial and error procedure.
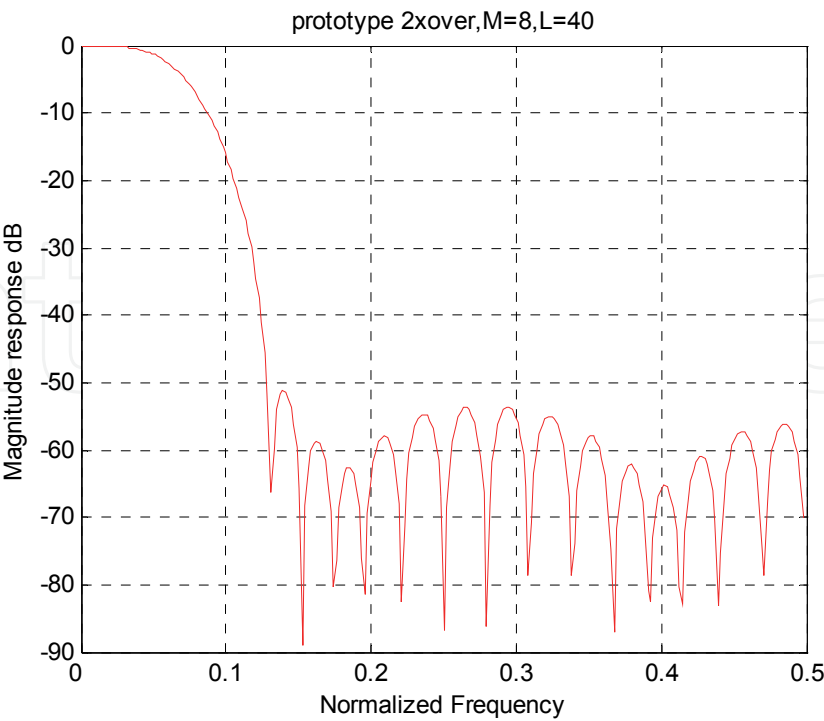
Fig. 9. Optimized prototype filter

3.4 Polyphse implementation of the subband noise canceller

The implementation of DFT modulated filter banks can be done using polyphase decomposition of a single prototype filter and a Fast Fourier Transform (FFT). A DFT modulated analysis filter bank with subsequent D-fold downsampling is implemented as a tapped delay line of size M with D-fold downsampling, followed by a structured matrix $M{\times}D$ containing the polyphase components of the analysis prototype filter $\mathbf{F}(z)$, and an $M{\times}M$ FFT matrix as shown in Fig. 10. The synthesis bank is constructed in a reversed fashion with $D{\times}M$ matrix containing the polyphase components of the synthesis filter bank $\tilde{\mathbf{F}}(z)$.

3.5 Results of the optimized 2-fold oversampled noise canceller

The noise path used in these tests is an approximation of a small room impulse response modeled by a FIR processor of 512 taps. To measure the convergence behavior of the oversampled subband noise canceller, a variable frequency sinusoid was corrupted with white Gaussian noise. This noise was passed through the noise path, and then applied to the primary input of the noise canceller, with white Gaussian noise is applied to the reference input. Experimental parameters are listed in Table 2. Mean square error convergence is used as a measure of performance. Plots of MSE are produced and smoothed with a suitable moving average filter. A comparison is made with a conventional fullband system as well as with a recently developed critically sampled system (Kim et al 2008) as shown in Fig.11. The optimized system is denoted by (OS), the critically sampled system is denoted by (CS) and the fullband system is denoted by (FB). To test the behavior under environmental conditions, a speech signal is then applied to the primary input of the proposed noise canceller. The speech was in the form of Malay

utterance "Kosong, Satu, Dua,Tiga" spoken by a woman. The speech was sampled at 16 kHz. Engine noise is used as a background interference to corrupt the above speech. Plots of MSE are produced as shown in Fig.12. In this figure, convergence plots of a fullband and critically sampled systems are also depicted for comparison.
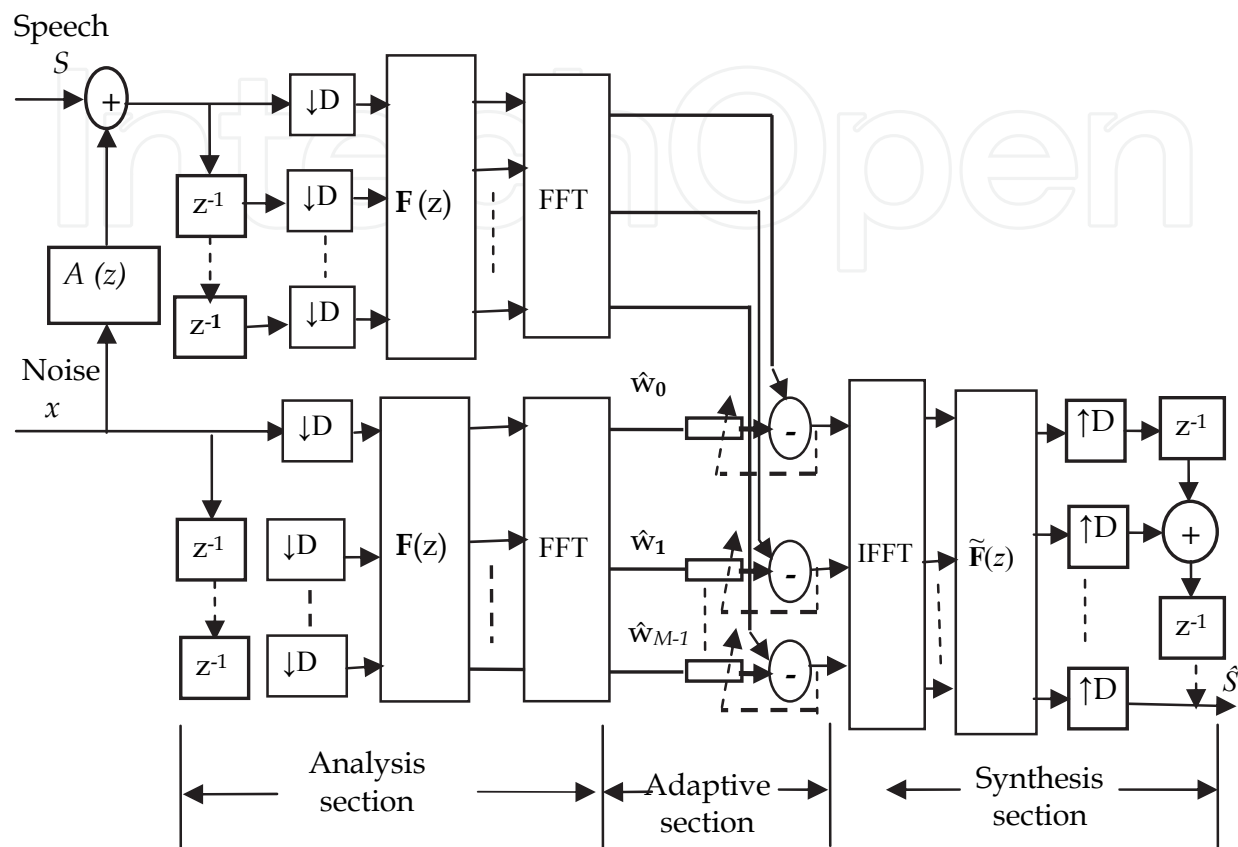

Fig. 10. Polyphase implementation of the multiband noise canceller

Parameter	Specification
Acoustic noise path	FIR processor with 512 taps
Adaptation algorithm type	Subband power normalized LMS
Primary input (first test)	Variable frequency sinusoid
Reference input (first test)	Additive white Gaussian noise
Primary input (second test)	Malay utterance, sampled at 16 kHz
Reference input (second test)	Machinery noise

Table 2. Test parameters

3.6 Discussion
From Figure 11, it is clear that the MSE plot of the proposed oversampled subband noise canceller converges faster than the fullband. While the fullband system is converging slowly, the oversampled noise canceller approaches 25 dB noise reductions in about 2500 iterations. In an environment where the impulse response of the noise path is changing over

a period of time shorter than the initial convergence period, initial convergence will most affect cancellation quality. On the other hand, the CS system developed using the method by (Kim et al. 2008) needs a longer transient time than that OS system. The FB canceller needs around 10000 iterations to reach approximately a similar noise reduction level. In case of speech and machinery noise (Fig12), it is clear that the FB system converges slowly with colored noise as the input to the adaptive filters. Tests performed in this part of the experiment proved that the proposed optimized OS noise canceller does have better performance than the conventional fullband model as well as a recently developed critically sampled system. However, for white noise interference, there is still some amount of residual error on steady state as it can be noticed from a close inspection of Fig.11.
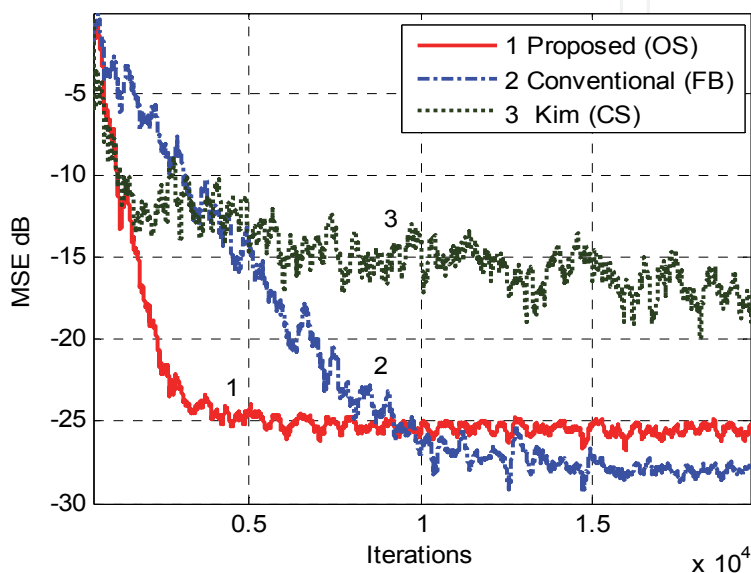
Fig. 11. MSE performance under white noise
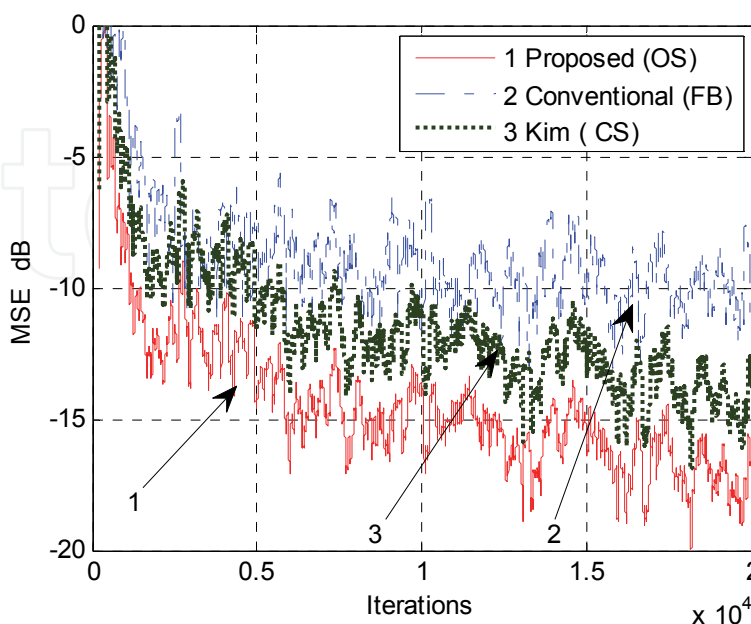
Fig. 12. MSE performance under environmental conditions

4. Low complexity noise cancellation technique

In the last section, optimized oversampled filter banks are used in the subband noise cancellation system as an appropriate solution to avoid aliasing distortion associated with the critically sampled subband noise canceller. However, oversampled systems imply higher computational requirements than critically sampled ones. In addition, it has been shown in the previous section that oversampled FIR filter banks themselves color the input signal, which leads to under modeling and hence high residual noise at system's output for white noise. Therefore, a cheaper implementation of the subband noise canceller that retains good   noise reduction performance and low signal delay is sought in this section. The idea is centered on using allpass infinite impulse response filters. The filters can be good alternatives for FIR filters. Flat responses with very small transition band, can be achieved with only few filter coefficients. Aliasing distortion in the analysis filter banks can be reduced to tolerable levels with lower expenses and acceptable delay. In literature, the use of allpass IIR filter banks for echo control has been treated by Naylor et al. (1998). One shortcoming of this treatment is the spectral gaps produced as a result of using notch filtering to preprocess the subband signals at the analysis stage in an attempt to reduce the effect of nonlinearity on the processed signal. The use of notch filters by Naylor et al. (1998) has also increased processing delay. In this section, an adaptive noise cancellation scheme that uses a combination of polyphase allpass filter banks at the analysis stage and an optimized FIR filter bank at the synthesis stage is developed and tested. The synthesis filters are designed in such a way that inherent phase correction is made at the output of the noise canceller. The adaptive process is carried out as given by equations (34)-(37). Details of the design of analysis and synthesis filter banks are described in the following subsections.

4.1 Analysis filter bank design
The analysis prototype filter of the proposed system is constructed from second order allpass sections as shown in Fig.13. The transfer function of the prototype analysis filter is given by

$$H_0(z) = \frac{1}{2}\sum_{k=0}^{N-1} F_k(z^{-2})z^{-k} \tag{38}$$

where,

$$F_k(z^{-2}) = \prod_{n=1}^{L_k} F_{k,n}(z^{-2}) = \prod_{n=1}^{L_k} \frac{\alpha_{k,n}+z^{-2}}{1+\alpha_{k,n}z^{-2}} \tag{39}$$

where $\alpha_{k,n}$ is the coefficient of the kth allpass section in the nth branch L_n is the number of sections in the nth branch, and N is the order of the section. These parameters can be determined from filter specifications. The discussion in this chapter is limited to second order allpass sections, since higher order allpass functions can be built from products of such second order filters.
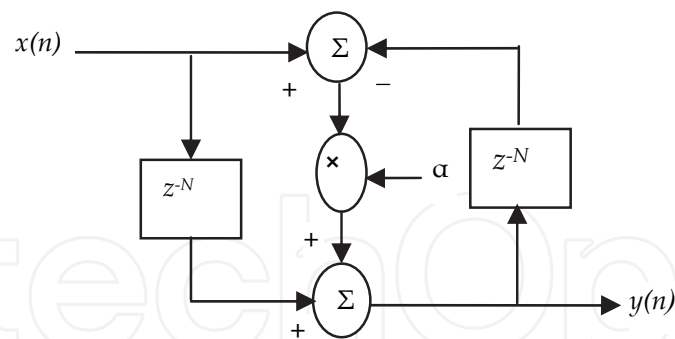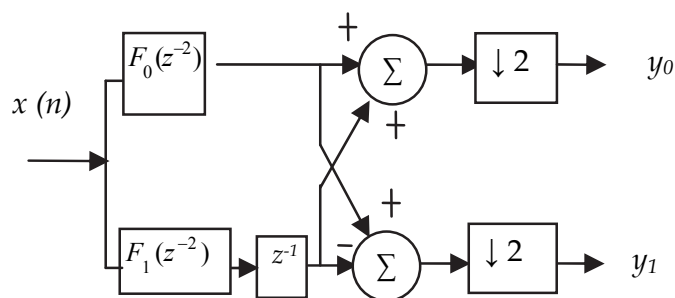
Fig. 13. The second order allpass section

Fig. 14. Polyphase implementation

Furthermore, to maintain the performance of the filters in fixed point implementation, it is advantageous to use cascaded first or second-order sections (Mendel 1991). These filters can be used to produce multirate filter banks with high filtering quality (Milić 2009). Elliptic filters fall into this class of filters yielding very low-complexity analysis filters (Poucki et al. 2010).The two band analysis filter bank that is shown on the L.H.S. of Fig.1 can be modified to the form of the polyphase implementation(type1) as shown in Fig.14 and is given by

$$H_0(z) = \frac{1}{2}(F_0(z^2) + z^{-1}F_1(z^2)) \tag{40}$$

$$H_1(z) = \frac{1}{2}(F_0(z^2) - z^{-1}F_1(z^2)) \tag{41}$$

Filters $H_0(z)$ and $H_1(z)$ are bandlimiting filters representing lowpass and highpass respectively. This modification results in half the number of calculations per input sample and half the storage requirements. In Fig.14, y_0 and y_1 represent lowpass and highpass filter outputs, respectively. The polyphase structure can be further modified by shifting the downsampler to the input to give more efficient implementation. According to the noble identities of multirate systems, moving the downsampler to the left of the filter results in the power of z in $F_0(z^2)$ and $F_1(z^2)$ to reduced to 1 and the filters becomes $F_0(z)$ and $F_1(z)$, where $F_0(z)$ and $F_1(z)$ are causal, real, stable allpass filters. Fig15 depicts the frequency response of the analysis filter bank.
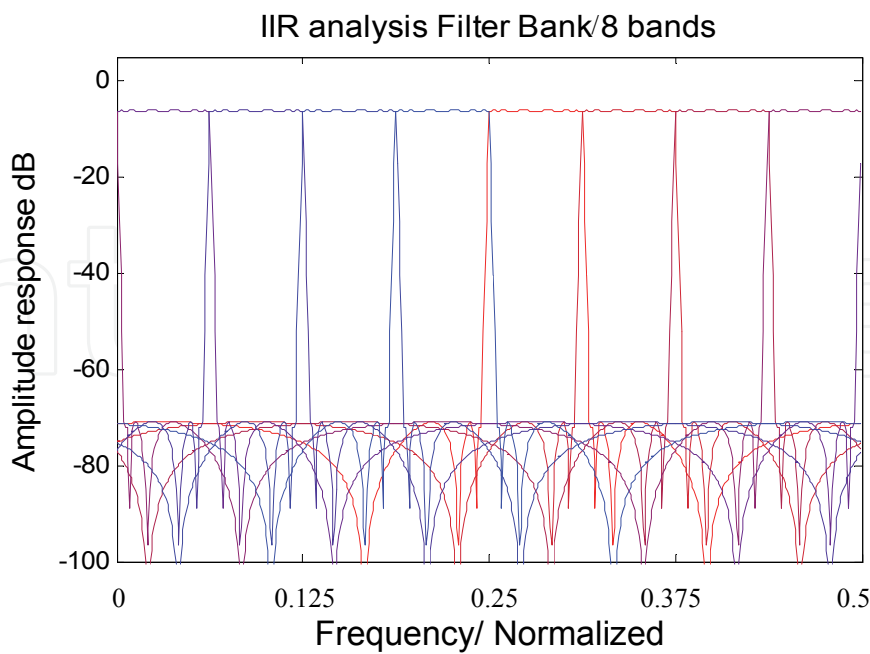
Fig. 15. Analysis filter bank magnitude frequency response

4.2 Analysis/synthesis matching

For phase correction at the noise canceller output, a relationship that relates analysis filters to synthesis filter is established as follows. The analysis prototype filter $H(z)$ can be represented in the frequency domain by,

$$H(e^{j\omega}) = \left| H(e^{j\omega}) \right| e^{j\varphi(\omega)} \tag{42}$$

where $\varphi(\omega)$ is the phase response of the analysis prototype filter. On the other hand, the synthesis filter bank is based on prototype low pass FIR filter that is related to the analysis prototype filter by the following relationship

$$G_d(e^{j\omega}) = \left| G_0(e^{j\omega}) \right| e^{j\psi} = \left| H_0(e^{j\omega}) \right| e^{-j[\omega.\partial + \varphi\,(\omega)]} \tag{43}$$

where $G_d(e^{j\omega})$ is the desired frequency response of synthesis prototype filter and ψ is the phase of the synthesis filter. This shall compensate for any possible phase distortion at the analysis stage. The coefficients of the prototype synthesis filter $G_d(e^{j\omega})$ are evaluated by minimizing the weighted squared of the error that is given by the following

$$WSE = \sum Wt(\omega) \left| G_0(e^{j\omega}) - G_{d.}(e^{j\omega}) \right|^2 \tag{44}$$

where $Wt(\omega)$ is a weighting function given by

$$Wt(\omega) = \left| \hat{G}_0(e^{j\omega}) - G_{d.}(e^{j\omega}) \right|^2 \tag{45}$$

where $\hat{G}_0(e^{j\omega})$ is an approximation of the desired frequency response, it is obtained by frequency transforming the truncated impulse response of the desired prototype filter, leading to nearly perfect reconstruction up to a delay in which the amplitude, phase and aliasing distortions will be small. *WSE* is evaluated on a dense grid of frequencies linearly distributed in the fundamental frequency range. The use of FIR filter bank at the synthesis stage with prototype filter as dictated by (43) ensures a linear phase at the output, a constant group delay and a good analysis/synthesis matching. Plot of the distortion function is shown in Fig. 16. It is obvious from this figure that the distortion due the filter bank is quite low.
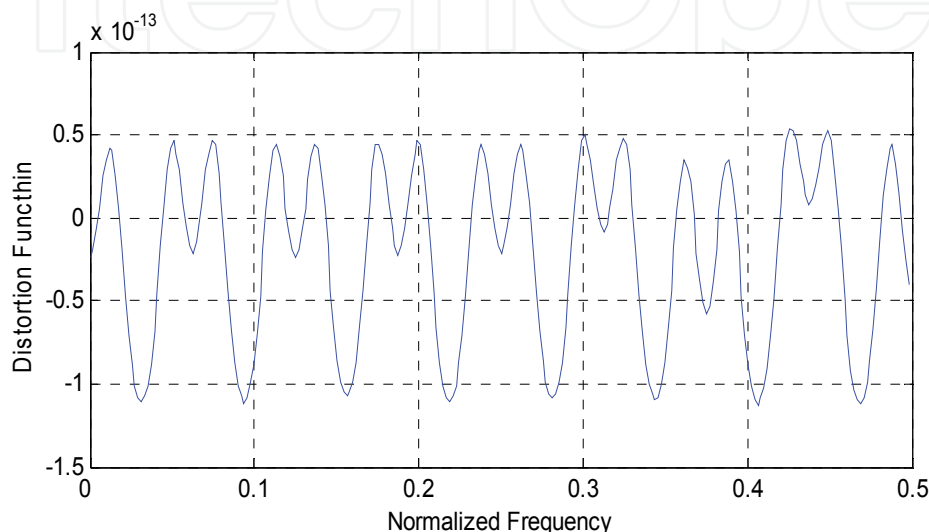
Fig. 16. Distortion function

4.3 Computational complexity and system delay analysis

The total computational complexity of the system can be calculated in three parts, analysis, adaptive and synthesis. The complexity of 8-band analysis filter bank with eight coefficients prototype filter, and for tree implementation of three stages giving a total of 28 multiplication operations per unit sample by utilizing the noble identities. The complexity of the adaptive section is calculated as the fullband adaptive filter length L_{FB} divided by the number of subbands, $L_{FB}/8$ .The complexity of the synthesis section is calculated directly by multiplying the number of filter coefficients by the number of bands, in our case, for 55 tap synthesis prototype filter, and for eight band filter bank, which gives a total to 440 multiplication operations at the synthesis stage. Therefore, the overall number of multiplication operations required is ($578+ L_{FB}/8$). Now, comparing with a system uses high order FIR filter banks at the analysis and the synthesis stages to give that equivalent performance. For an equivalent performance, the length of the prototype should be at least 128, and for 8 bands, at the analysis stage we need 1024 multiplication operations, a similar number at the synthesis stage is required. Thus, for two analysis filter banks and one synthesis filterbank total number of multiplications $=2048+ L_{FB}/8$. On the other hand, the computational complexity of block updating method given by Narasimha (2007) requires three complex FFT operations, each one corresponds to $2\times L_{AF}\times\log_2 L_{AF} - L_{AF}$ multiplications, which is much higher than the proposed method. In acoustic environments,

the length of the acoustic path usually few thousands of taps, making the adaptive section is the main bulk of computations. As far as system delay is concerned, the prototype analysis filter has a group delay between 2.5 and 5 samples except at the band edge where it reaches about 40 samples as shown in Fig. 17. The maximum group delay due to the analysis filter bank is 70 samples calculated as 40 samples for the first stage followed by two stages, each of them working at half the rate of the previous one. The synthesis stage has a maximum group delay of 27 samples which brings the total delay to 97 samples..
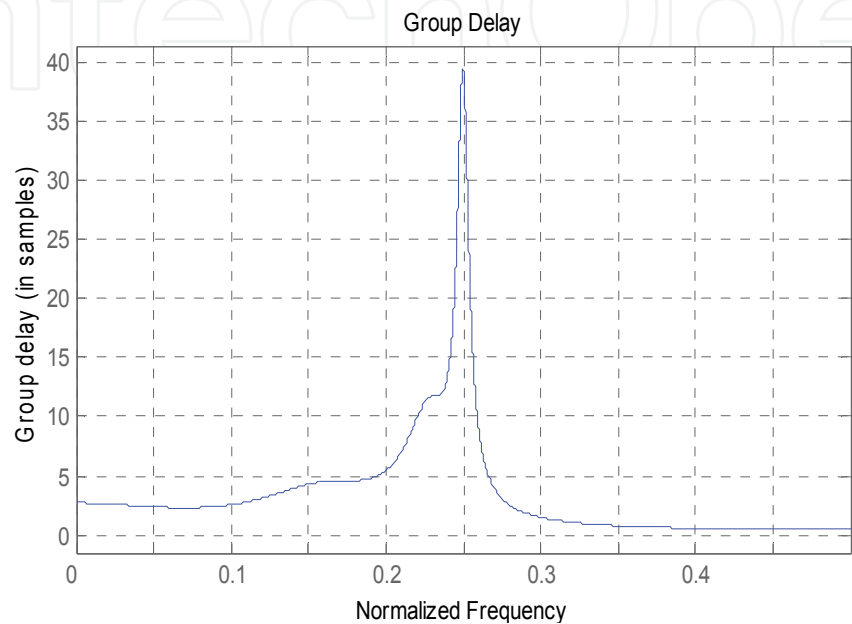
Fig. 17. Group delay of prototype analysis filter

In the technique offered by Narasimha (2007) for example, the output is calculated only after the accumulation of L_{FB} samples block. For a path length of 512 considered in these experiments, a delay by the same amount of samples is produced, which is higher than the proposed one, particularly if a practical acoustic path is considered. Therefore for tracking non-stationary signals our proposed technique offers a better tracking than that offered by Narasimha (2007). Furthermore, comparison of computational complexity of our LC system with other literature techniques is depicted in table 3.

	Kim (2008)	Narasimha (2007)	Choi&Bai (2007)	Proposed (LC)
Complexity	890	27136	2056	532
Delay/samples	430	512	128	97

Table 3. Computational complexity and delay comparison.

4.4 Results and discussion of the low complexity noise canceller

The same input signals and noise path as in in previous section are used in testing the low complexity system. In the sequel, the following notations shall be used, LC for low complexity noise canceller, OS and FB stand for oversampled and fullband systems, respectively. It is shown in Fig. 18 that mean square error plots of the OS system levels off

at -25 dB after a fast initial convergence. This due to the presence of colored components as discussed in the last section. Meanwhile, the MSE plot of the proposed LC noise canceller outperforms the MSE plot of the classical fullband system during initial convergence and exhibits comparable steady state performance with a little amount of residual noise. This is probably due to some non linearity which may not be fully equalized by the synthesis stage, since the synthesis filter bank is constructed by an approximation procedure. However, subjective tests showed that the effect on actual hearing is hardly noticed. It is obvious that the LC system reaches a steady state in approximately 4000 iterations. The fullband (FB) system needs more than 10000 iterations to reach the same noise cancellation level. On the other hand, the amount of residual noise has been reduced compared to the OS FIR/FIR noise canceller. Tests performed using actual speech and ambient interference (Fig. 19) proved that the proposed LC noise canceller does have an improved performance compared to OS scheme, as well as the FB canceller. The improvement in noise reduction on steady state ranges from 15-20 dB compared to fullband case, as this is evident from Fig. 20. The improved results for the proposed LC system employing polyphase IIR analysis filter bank can be traced back to the steeper transition bands, nearly perfect reconstruction, good channel separation and very flat passband response, within each band. For an input speech sampled at 16 kHz, the adaptation time for the given channel and input signal is measured to be below 0.8 seconds. The convergence of the NLMS approaches above 80% in approximately 0.5 seconds. The LC noise canceller possesses the advantage of low number of multiplications required per input sample. To sum up, the proposed LC approach showed an improved performance for white and colored interference situations, proving usefulness of the method for noise cancellation.
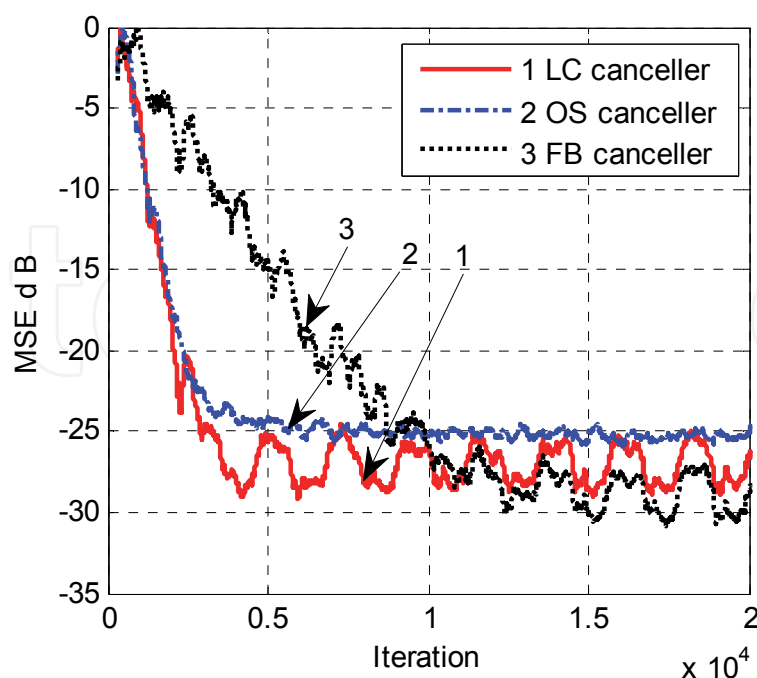

Fig. 18. MSE performance comparison of the proposed low complexity (LC) system with an equivalent oversampled (OS) and fullband (FB) cancellers under white noise interference
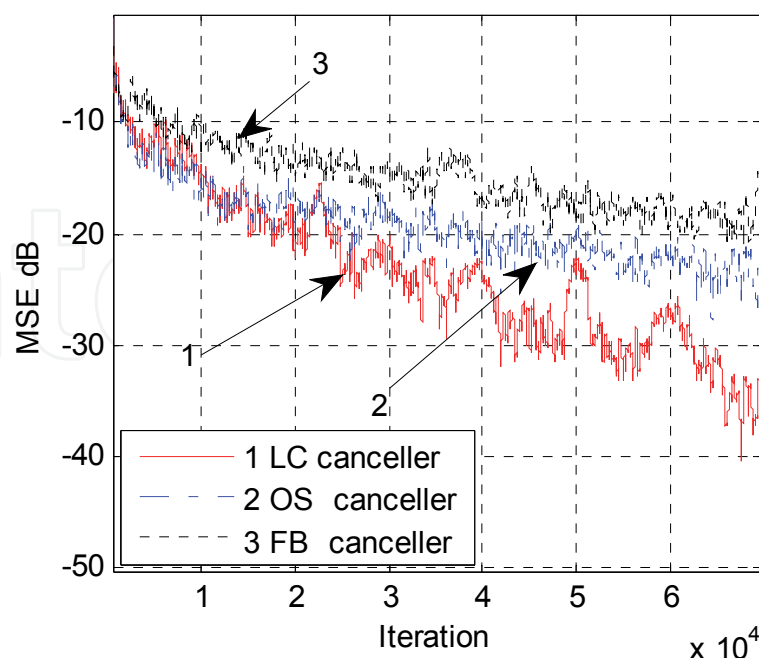
Fig. 19. MSE performance comparison of the proposed low complexity (LC) system with an equivalent oversampled (OS) and conventional fullband (FB) cancellers under ambient noise

5. Conclusion

Adaptive filter noise cancellation systems using subband processing are developed and tested in this chapter. Convergence and computational advantages are expected from using such a technique. Results obtained showed that; noise cancellation techniques using critically sampled filter banks have no convergence improvement, except for the case of two-band QMF decomposition, where the success was only moderate. Only computational advantages may be obtained in this case. An improved convergence behavior is obtained by using two-fold oversampled DFT filter bank that is optimized for low amplitude distortion. The price to be paid is the increase in computational costs. Another limitation with this technique is the coloring effect of the filter bank when the background noise is white. The use of polyphase allpass IIR filters at the analysis stage with inherent phase compensation at the synthesis stage have reduced the computational complexity of the system and showed convergence advantages. This reduction in computational power can be utilized in using more subbands for high accuracy and lower convergence time required to model very long acoustic paths. Moreover, the low complexity system offered a lower delay than that offered by other techniques. A further improvement to the current work can be achieved by using a selective algorithm that can apply different adaptation algorithms for different frequency bands. Also, the use of other transforms can be investigated.

6. References

Bergen, S.W.A. (2008). A design method for cosine-modulated filter banks using weighted constrained-least-squares filters, *Elsevier Signal Processing Journal*, Vol.18, No.3, (May 2008), pp. 282–290. ISSN 1051-2004.

Choi, H, & Bae, H.D. (2007). Subband affine projection algorithm for acoustic echo cancellation system. *EURASIP Journal on Advances in Signal Processing*, Vol. 2007. doi:10.1155/2007/75621, ISSN 1110-8657.

Deng, Y.; Mathews, V.J. & Boroujeny, B.F. (2007). Low-Delay Nonuniform Pseudo-QMF Banks With Application to Speech Enhancement, *IEEE Trans. on Signal Processing*, Vol.55, No.5, (May 2007), pp. 2110-2121, ISSN 1053-587X.

Diniz, P. S. R. (2008). *Adaptive Filtering: Algorithms and practical implementations 3rd edition*, Springer Science+Business Media, ISBN 978-0-387-3-31274-3, New York, USA.

Hameed, A.K.M. & Elias, E. (2006). M-channel cosine modulated filter banks with linear phase analysis and synthesis filters. *Elsevier Signal Processing,* Vol.86, No.12, December 2006, pp. 3842–3848.

Haykin, S. (2002). *Adaptive filter Theory*, 4thed, Prentice Hall, ISBN 0-130-90126-1, New Jersey, USA.

Hoge, S.W.; Gallego, F.; Xiao, Z. & Brooks. D.H. (2008). RLS-GRAPPA: Reconstructing parallel MRI data with adaptive filters, *Proceedings of the 5th IEEE Symposium on Biomedical Imaging* (ISBI 2008), pp. 1537-1540, ISBN 978-1-4244-2002-5,Paris, France, May 14-17, 2008.

Johnson, J.; Cornu, E.; Choy G. & Wdowiak, J. (2004). Ultra low-power sub-band acoustic echo cancellation for wireless headsets, *Proceedings of the IEEE International Conference on Acoustics, Speech and Signal Processing*, pp. V357-60, ISBN 0-7803-8484-9, Montreal, Canada, May 17-21, 2004.

Kim, S.G., Yoo, C.D. & Nguyen, T.Q. (2008). Alias-free subband adaptive filtering with critical sampling. *IEEE Transactions on Signal Proces*sing. Vol.56, No.5, May 2008, pp. 1894-1904. ISSN 1053-587X.

Lin, X.; Khong, A. W. H.; Doroslova˘cki, M. & Naylor, P. A. (2008). Frequency-domain adaptive algorithm for network echo cancellation in VoIP. *EURASIP Journal on Audio, Speech, and Music Processing.* Volume 2008, Article ID 156960, 9 pages, doi:10.1155/2008/156960, ISSN 1687-4714.

Martinez, J.I.M., & Nakano, K. (2008). Cascade lattice IIR adaptive filter structure using simultaneous perturbation method for self-adjusting SHARF algorithm, *Proceedings of* SICE *Annual SICE Annual Conference,* pp. 2156-2161, ISBN 978-4-907764-30-2, Tokyo, Japan, 20-22 August 20-22, 2008.

Mendel, J.M. (1991). Tutorial on higher-order statistics (spectra) in signal processing and system theory: Theoretical results and some applications. *IEEE Transactions*, (March 1991), Vol. 79, No.3, pp. 278–305, ISSN 0018-9219.

Milić, L. (2009). *Multirate filtering for digital signal processing: MATLAB Applications*. Information Science Reference (IGI Global), ISBN 1605661783, Hershy PA 17033, USA.

Narasimha, M.J. (2007). Block adaptive filter with time-domain update using three transforms. *IEEE Signal Processing Letters*, Vol.14, No.1, (January 2007), pp51-53, ISSN 1070-9908.

Naylor, P.A., Tanrıkulu,O. & Constantinides, A.G. (1998). Subband adaptive filtering for acoustic echo control using allpass polyphase IIR filterbanks. *IEEE Transactions on Speech and Audio Processing,* Vol.6, No.2, (March 1998), pp. 143-155. ISSN 1063-6676.

Nguyen, T. Q. & Vaidyanathan, P.P. (1988). Maximally decimated perfect – reconstruction FIR filter banks with pairwise mirror-Image analysis (and synthesis) frequency

response. *IEEE Trans. on Acoustics, Speech and Signal Processing, Vol.*36, No.5, (May 1988), pp. 693-706. ISSN 0096-3518.

Poucki , V.M.;   Žemvaa, A. ; Lutovacb, M.D. &   Karcnik, T. (2010). Elliptic IIR filter sharpening implemented on FPGA. *Elsevier Signal Processing,* Vol.20, No.1, (January 2010), pp. 13–22, ISSN 1051-2004.

Radenkovic, M. & Tamal Bose. (2001). Adaptive IIR filtering of non stationary signals. *Elsevier Signal Processing,* Vol.81, No.1, (January 2010), pp.183-195, ISSN 0165-1684.

Vaseghi, V.S. (2008). *Advanced digital signal processing and noise reduction.* 4rd Edition, John Willey and Sons Ltd, 978-0-470-75406-1, West Sussex, England.

Wasfy, M., B. & Ranganathan, R. 2008. Complex FIR block adaptive digital filtering algorithm with independent adaptation of real and imaginary filter parameters, *Proceedings of the 51st Midwest Symposium on Circuits and Systems*, pp. 854-85, ISBN 978-1-4244-2166-4, Knoxville, TN, August 10-13, 2008.

Adaptive Filtering

Edited by Dr Lino Garcia

Adaptive filtering is useful in any application where the signals or the modeled system vary over time. The configuration of the system and, in particular, the position where the adaptive processor is placed generate different areas or application fields such as prediction, system identification and modeling, equalization, cancellation of interference, etc., which are very important in many disciplines such as control systems, communications, signal processing, acoustics, voice, sound and image, etc. The book consists of noise and echo cancellation, medical applications, communications systems and others hardly joined by their heterogeneity. Each application is a case study with rigor that shows weakness/strength of the method used, assesses its suitability and suggests new forms and areas of use. The problems are becoming increasingly complex and applications must be adapted to solve them. The adaptive filters have proven to be useful in these environments of multiple input/output, variant-time behaviors, and long and complex transfer functions effectively, but fundamentally they still have to evolve. This book is a demonstration of this and a small illustration of everything that is to come.

INTECH
open science | open minds